



Undifferentiated HepaRG cells show reduced sensitivity to the toxic effects of M8OI through a combination of CYP3A7-mediated oxidation and a reduced reliance on mitochondrial function

Tarek M. Abdelghany^{b,c}, Shireen A. Hedy^{b,a}, Alex Charlton^d, Fahad A. Aljehani^{a,e}, Khalid Alanazi^a, Alaa A. Budastour^a, Larissa Marin^a, Matthew C. Wright^{a,*}

^a Translational and Clinical Research Institute, Newcastle University, Newcastle Upon Tyne, NE2 4AA, United Kingdom

^b Department of Pharmacology and Toxicology, Faculty of Pharmacy, Cairo University, Kasr El-Aini St., Cairo, 11562, Egypt

^c Institute of Education in Healthcare and Medical Sciences, School of Medicine, Medical Sciences and Nutrition, University of Aberdeen, Forehill, Aberdeen, AB25 2ZD, United Kingdom

^d School of Natural and Environmental Sciences, Bedson Building, Newcastle University, NE1 8QB, United Kingdom

^e Biochemistry Department, Faculty of Science, King Abdulaziz University, Jeddah, Saudi Arabia

ARTICLE INFO

Handling Editor: Dr. Bryan Delaney

Keywords:
Ionic liquids
C8mim
Cytochrome p450
AR42J-B13
Galactose
Lactate

ABSTRACT

The methylimidazolium ionic liquid M8OI (1-octyl-3-methylimidazolium chloride, also known as [C8mim]Cl) has been detected in the environment and may represent a hazard trigger for the autoimmune liver disease primary biliary cholangitis, based in part on studies using a rat liver progenitor cell. The effect of M8OI on an equivalent human liver progenitor (undifferentiated HepaRG cells; u-HepaRG) was therefore examined. u-HepaRG cells were less sensitive (>20-fold) to the toxic effects of M8OI. The relative insensitivity of u-HepaRG cells to M8OI was in part, associated with a detoxification by monooxygenation via CYP3A7 followed by further oxidation to a carboxylic acid. Expression of CYP3A7 - in contrast to the related adult hepatic CYP3A4 and CYP3A5 forms - was confirmed in u-HepaRG cells. However, blocking M8OI metabolism with ketoconazole only partly sensitized u-HepaRG cells. Despite similar proliferation rates, u-HepaRG cells consumed around 75% less oxygen than B-13 cells, reflective of reduced dependence on mitochondrial activity (Crabtree effect). Replacing glucose with galactose, resulted in an increase in u-HepaRG cell sensitivity to M8OI, near similar to that seen in B-13 cells. u-HepaRG cells therefore show reduced sensitivity to the toxic effects of M8OI through a combination of metabolic detoxification and their reduced reliance on mitochondrial function.

1. Introduction

Methylimidazolium ionic liquids (MILs) are man-made solvents used in industrial processes such as biofuel production (Deyab and Mohsen, 2021; Poolakkalody et al., 2022). They comprise a methylimidazolium cation moiety and an alkyl chain of variable length, combined with an anion (which may be anything from chloride ion to a variety of more complex anions). Short alkyl (2C and 4C) chain MILs are most used in the EU (Leitch et al., 2020a). Recent work from this laboratory detected an 8C MIL cation (i.e. 1-octyl-3-methylimidazolium, also known as C8mim - for structure see Fig. 1a) in the environment and in 6 out of 30 serum samples randomly-selected from a liver patient biobank (Probert et al., 2018; Leitch et al., 2020a, 2021). This suggests that there may be an escape of MILs into the environment, leading to

human population exposure.

Detection of M8OI (specifically referring to the Cl⁻ salt) in the environment was originally identified using cell-based effect screens (Probert et al., 2018). The cell employed to screen for toxicity at that time was the rat hepatic progenitor B-13 cell line and, after confirming M8OI as the cause of toxicity, subsequent studies have continued to use the cell line to examine toxicity mechanisms (Abdelghany et al., 2020; Hedy et al., 2023). The B-13:B-13/H model is a platform technology that has been available for over 20 years. It consists of a proliferative rat progenitor B-13 cell line which can be readily expanded and used to generate replicatively-senescent hepatocyte-like B-13/H cells (Wallace et al., 2010; Probert et al., 2015). Trans-differentiation to the B-13/H phenotype requires treatment with glucocorticoid. The process appears to be associated with a pathological response that can occur in vivo (Wallace et al., 2010a, 2010b). In B-13 cells, trans-differentiation is

* Corresponding author. Translational and Clinical Research Institute, Level 4 Leech, Newcastle University, Newcastle Upon Tyne, NE24HH, United Kingdom.
E-mail address: m.c.wright@ncl.ac.uk (M.C. Wright).

<https://doi.org/10.1016/j.fct.2024.114681>

Received 6 February 2024; Received in revised form 15 April 2024; Accepted 21 April 2024

Available online 25 April 2024

0278-6915/© 2024 The Authors. Published by Elsevier Ltd. This is an open access article under the CC BY license (<http://creativecommons.org/licenses/by/4.0/>).

Abbreviations

B-13	AR42J-B13 cell line	MIL	methylimidazolium ionic liquid
B-13/H	hepatocyte-like cells derived from B-13 cells	MO	monooxygenases(s)
COOH7IM	1-(7-carboxyheptyl)-3-methyl-1H-imidazole-3-ium	MTT	methylthiazolyldiphenyl-tetrazolium bromide
DCFDA	dichlorodihydrofluorescein diacetate	M8OI	1-octyl-3-methylimidazolium (also often referred to as C8mim)
DH	dehydrogenase	OCR	oxygen consumption rate
ECAR	extracellular acidification rate	PBC	primary biliary cholangitis
FCCP	carbonyl cyanide-4 (trifluoromethoxy) phenylhydrazone	PBS	phosphate buffered saline
FCS	fetal calf serum	PDC-E2	E2 component of the mitochondrial enzyme, pyruvate dehydrogenase
HO8IM	1-(8-Hydroxyoctyl)-3-methyl-imidazolium	ROS	reactive oxygen species
LDH	lactate dehydrogenase	u-HepaRG	HepaRG cells in their expansion, non-differentiated phenotype.
M8OI	1-octyl-3-methylimidazolium		

driven by a serum and glucocorticoid kinase 1-dependent block in Wnt signalling and induction of liver-specific transcription factors such as C/EBP β . For a review, see [Probert et al. \(2015\)](#). The mode of toxic action of M8OI appears to be similar in all cell types examined and involves a block in mitochondrial oxidative phosphorylation, likely through interactions upstream of complex III ([Abdelghany et al., 2020](#)). The inhibition in oxidative phosphorylation leads to an increase in medium glucose consumption and lactate production, suggestive of a compensatory increase in glycolysis ([Abdelghany et al., 2020](#)). Accordingly, provision of additional glucose to B-13 cells treated with M8OI was the most effective way of ameliorating M8OI toxicity ([Probert et al., 2018](#)).

We have recently proposed that M8OI may be hazard for initiating the auto-immune liver disease primary biliary cholangitis (PBC) ([Probert et al., 2018](#); [Leitch et al., 2020a](#)), a disease thought to be triggered by exposure to xenobiotics ([Triger, 1980](#); [Prince et al., 2001](#); [Ala et al., 2006](#); [Arsenijevic et al., 2016](#); [Hirschfield et al., 2018](#)). This is, in part, because the hepatic oxidative metabolite of M8OI – COOH7IM – can be enzymatically incorporated into the protein to which PBC patients lose tolerance ([Probert et al., 2018](#)). However, M8OI also induces both oxidative stress and an apoptotic mode of cell death in B-13 cells ([Abdelghany et al., 2020](#)), is estrogenic ([Leitch et al., 2018](#)) and is capable of inducing a cholestatic-type of liver injury in mice ([Leitch et al., 2020b](#)), features that would increase its chances of behaving as a trigger for PBC.

In order to examine the relevance of our observations made in experimental animal systems, the potential toxic effects of M8OI in human cells was considered. The HepaRG cell is a human liver-derived line that in response to glucocorticoid, differentiates into a mixed culture of cholangiocyte-like and hepatocyte-like cells ([Aninat et al., 2006](#); [Stanley and Wolf, 2022](#)). To our knowledge, the HepaRG cell line is the only cell line that behaves similarly to B-13 cells, in terms of functioning as an hepatocyte progenitor. Since the B-13 progenitor cell is more sensitive to M8OI than its hepatocyte-like derivative ([Probert et al., 2018](#); [Hedya et al., 2023](#)) and because liver progenitors also differentiate into cholangiocytes – the cell type classically associated with PBC – the undifferentiated HepaRG cell (designated u-HepaRG cells; summarised in [Fig. 1b](#)) was considered the optimum human system in which to study M8OI effects potentially relevant to PBC. Note, that this study deals solely with M8OI effects to u-HepaRG cells (i.e. in their progenitor phenotype). The basis of this study is hazard identification in a human system in vitro. Accordingly, the concentration ranges chosen is determined by effect rather than chosen to reflect realistic human exposure scenarios.

We demonstrate that u-HepaRG cells are relatively insensitive to the toxic effects of M8OI compared to B-13 cells and that this is not appreciably due to the higher levels of glucose used in the medium recommended for HepaRG propagation. Rather, u-HepaRG insensitivity appears to be associated with CYP3A7-mediated metabolism of M8OI in combination with a reduced reliance on mitochondrial oxidative

phosphorylation (Crabtree effect), when compared to B-13 cells. Although u-HepaRG cells are less sensitive to M8OI, they undergo apoptosis at sufficiently high concentrations of M8OI exposure and, given their capability to metabolise M8OI to the COOH7IM metabolite that can replace lipoic acid in PDC-E2, provide a human model system in which to examine potential PBC antigen production and presentation.

2. Methods

2.1. Materials

M8OI (purity >96%), CAS # 64697-40-1, was purchased from Sigma (Poole, UK). HepaRG cells were obtained from INSERM Transfert SA (Biopark Paris, France via Biopredic). Super somes were supplied by Corning, UK.

2.2. Cell culture

HepaRG cells were routinely cultured in Williams' E medium (containing 11 mM glucose) supplemented with 10% (v/v) fetal calf serum (FCS), 100 units/mL penicillin and 100 μ g/mL streptomycin, 5 μ g/mL insulin, 500 nM hydrocortisone hemisuccinate sodium salt and 0.584 g/L L-glutamine. B-13 cells and MCF-7 cells were cultured in low glucose (1 g/L, 5 mM) Dulbecco's Modified Eagle's Medium (DMEM) containing 10% (v/v) FCS, 100 units/ml penicillin, 100 mg/ml streptomycin and 0.584 g/L L-glutamine. Conversion to B-13 cells to B-13/H cells was achieved through addition of 10 nM dexamethasone to medium. Conversion of u-HepaRG cells to a mixture of hepatocyte-like and cholangiocyte-like cells was achieved through addition of 50 μ M hydrocortisone hemisuccinate sodium salt to the medium. The cells were then maintained with medium changes every 2–3 days - without sub-culture – for 2–3 weeks. Cells were cultured at 37 °C in an humidified incubator gassed with 5% CO₂ in air. Media were replenished every 2–3 days.

M8OI was prepared as 1000-fold molar concentrated stocks in sterile water and 0.1% (v/v) sterile water added to cells as control. All other compounds were prepared as 1000-fold molar concentrated stocks in DMSO and 0.1% (v/v) DMSO added to cells as control.

2.3. MTT assay

Methylthiazolyldiphenyl-tetrazolium bromide (MTT) reduction ([Van de Loosdrecht et al., 1994](#)) was determined as a surrogate for cell viability essentially as previously examined ([Hedya et al., 2023](#)). Results are presented as percentage MTT reduction relative to vehicle control-treated cells.

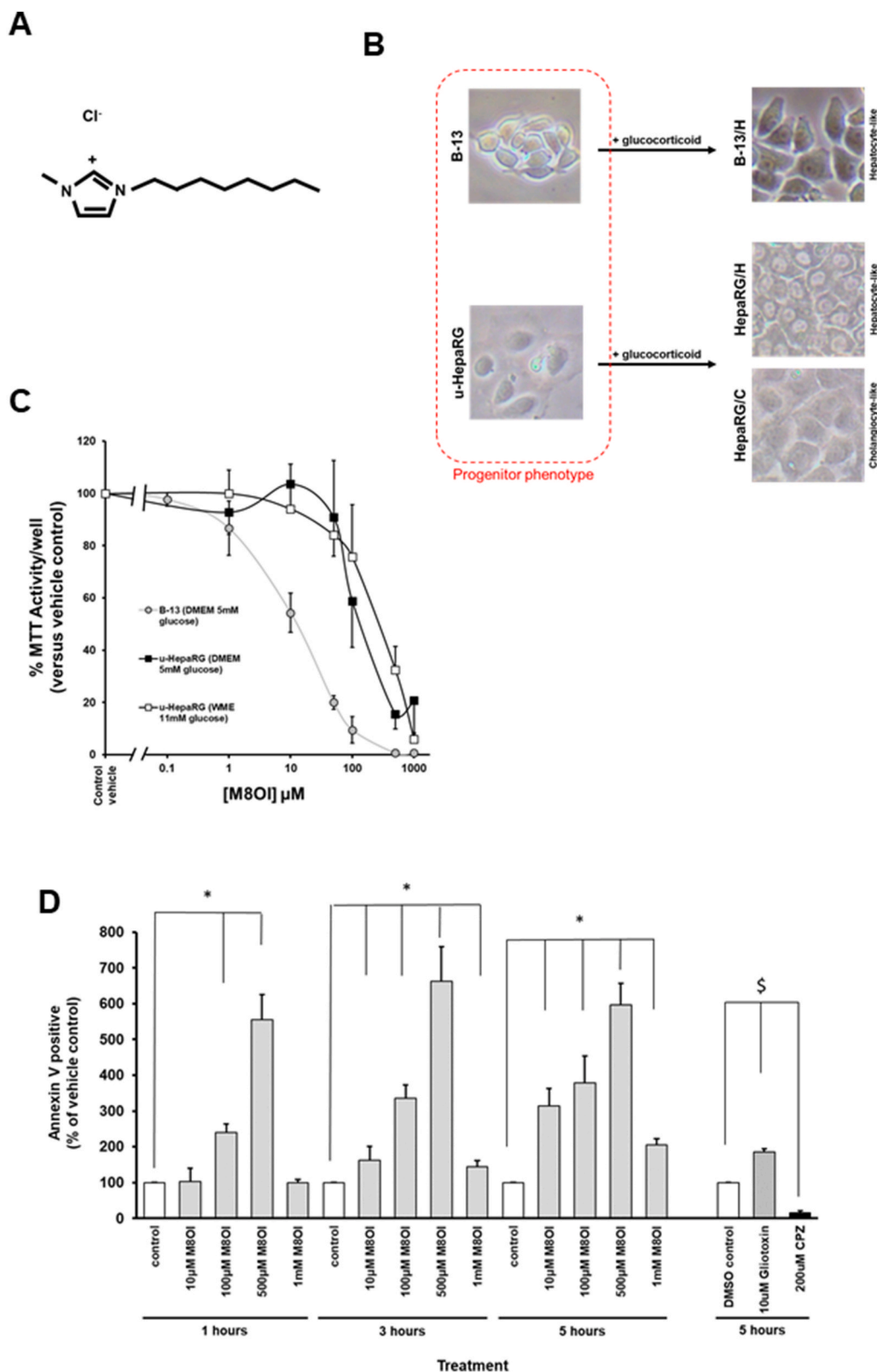


Fig. 1. u-HepaRG cells undergo an apoptotic mode of cell death in response to M8OI. **A**, structure of M8OI, note that this abbreviation refers specifically to the chloride salt. Since chloride is a common anion present at high concentrations in biological systems, it provides the optimum salt variant in which to study toxicity associated solely with the cation. A variety of other anions may be used with MILs (Leitch et al., 2020a) which may themselves also be toxic. **B**, schematic comparison of the effects of glucocorticoid on the differentiation status of B-13 and u-HepaRG cells. Note, this study only examines the effects of M8OI on the cell types enclosed within the dotted red line. **C**, Effects of M8OI on the viability of B-13 and u-HepaRG cells based on MTT reduction after 24 h. Data are the mean and SD of 4 separate determinations, typical of at least 10 separate experiments. LC_{50} for M8OI in B-13 cells, $12 \pm 4.4 \mu\text{M}$; for u-HepaRG cells in DMEM, $100 \pm 29 \mu\text{M}$ and for u-HepaRG cells in WME, $460 \pm 212 \mu\text{M}$. **D**, Effects of M8OI on Annexin V/phosphatidylserine-dependent luminescence in live u-HepaRG cells at the indicated exposure times. Data are the mean and SD of 6 separate determinations, typical of at least 3 separate experiments. **E**, Effects of M8OI on active caspase 3/7 activities in u-HepaRG

cells at the indicated exposure times. Data are the mean and SD of 3 separate determinations, typical of at least 6 separate experiments. **F**, Effects of M8OI on lactate dehydrogenase leakage in u-HepaRG cells at the indicated exposure times. Data are the mean and SD of 4 separate determinations, typical of at least 3 separate experiments. **G**, Effects of M8OI on the viability of u-HepaRG cells based on trypan blue exclusion after 24 h. Typical phase contrast views (large panels) of cells treated as indicated, black bar = 100 μ m. Inset panels, typical bright light images of cells treated with trypan blue, white bar = 20 μ m. **H**, Ethidium bromide gel electrophoresis of DNA isolated from cells treated as indicated for 24 h. Typical of at least 3 separate experiments. Control, 0.1% (v/v) water to control for solvent vehicle used for M8OI; DMSO control, 0.1% DMSO (v/v) to control for solvent vehicle used for other chemicals, CPZ, chlorpromazine; SP, staurosporine. Statistically significantly different (two tailed) from controls using one way ANOVA*, followed by a Tukey's post hoc test or Student's T test^S for 2 group comparisons ($p < 0.05$).

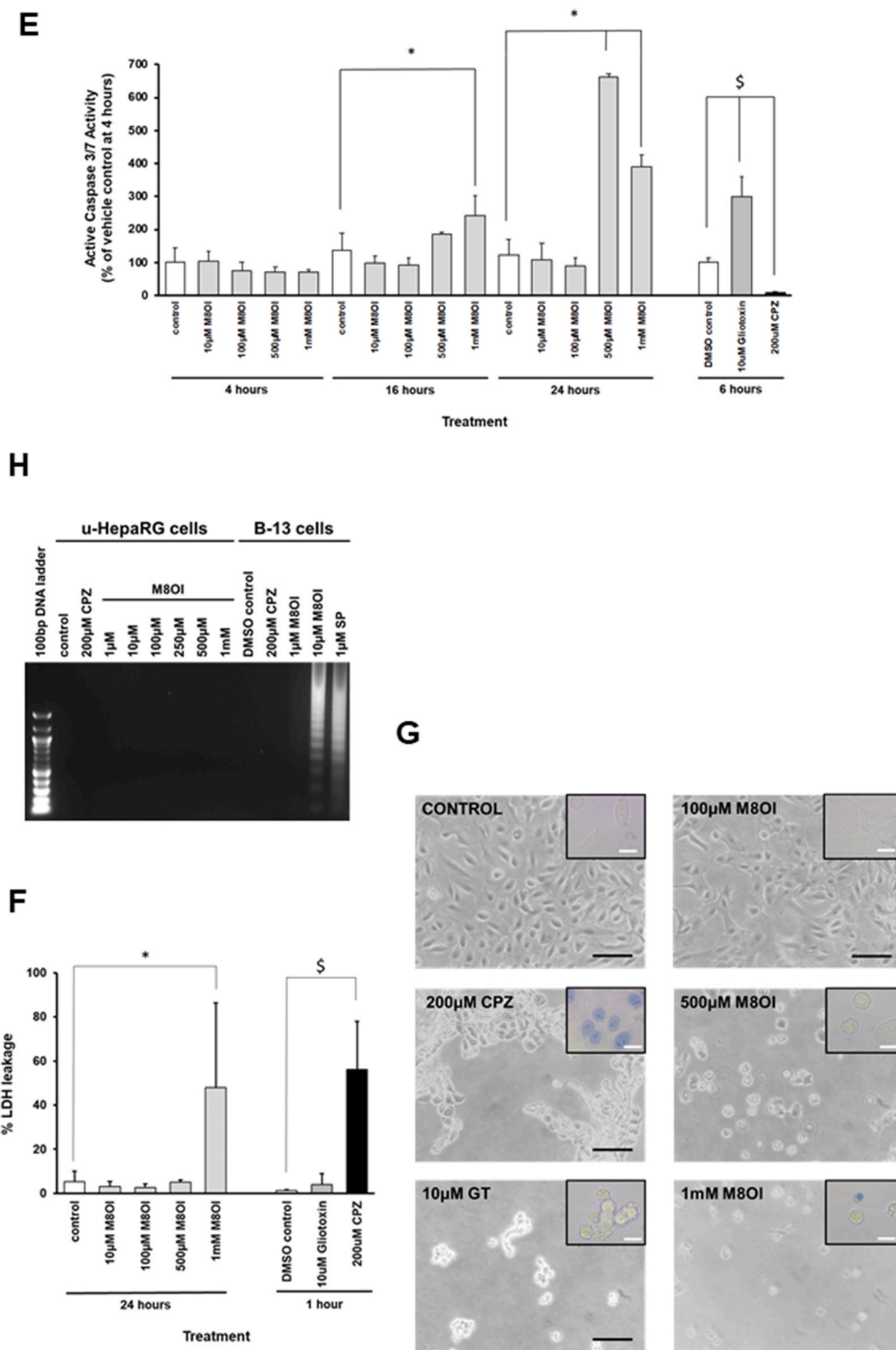


Fig. 1. (continued).

2.4. Surface localisation of phosphatidylserine using Annexin V

The localisation of phosphatidylserine on the external leaflet of the plasma membrane bilayer was determined using a RealTime-Glo™ Annexin V Apoptosis and Necrosis Assay kit (Promega, UK) for live cells essentially according to the manufacturer's instructions.

2.5. Active caspase 3/7 assays

Caspase activities were determined using Caspase-Glo® 3/7 assay kit (Promega, Southampton, UK) essentially following the manufacturer's instructions. Luminescence was recorded using a plate-reading luminometer (Berthold technologies).

2.6. Lactate dehydrogenase (LDH) leakage assay

LDH leakage was determined through examination of activities in culture media and cell lysates. Cell lysates were prepared after removal of medium and incubation of attached cells for 10 min with 10% (w/v) Triton X100 in H₂O essentially as previously determined (Hedya et al., 2023).

2.7. Nucleosomal DNA ladder

Genomic DNA was isolated and examined for DNA laddering by ethidium bromide agarose gel electrophoresis essentially as previously described (Wright et al., 2001).

2.8. Western blotting

Western blotting was performed essentially as previously described (Wallace et al., 2010a). Rabbit antisera against CYP3A4, CYP3A5 and CYP3A7 were a gift from Dr Rob Edwards (Imperial College, London, UK). An antibody against CYP1A1 was purchased from Abcam (Ab3568). Anti-β-actin (mouse monoclonal IgG cat #A1978) was obtained from Merck, UK. Blots were sequentially incubated with an appropriate species-specific HRP-conjugated anti-IgG followed by ECL detection and x-ray film exposure.

2.9. LC-MS analysis

M8OI and M8OI metabolites (HO8IM, COOH7IM) were quantified by standard multiple reaction monitoring (MRM) techniques using a Waters Xevo TQ-S Triple Quadrupole Mass-Spectrometer coupled to a Waters Acquity UPLC system. Separation was achieved by gradient elution with (A) 0.1% formic acid in water and (B) 0.1% formic acid in acetonitrile at a flow rate of 250 μL/min [5 % B at t = 0; 30 % B at t = 5 min; 95 % B at t = 8 min; 95 % B at t = 9 min; 5 % B at t = 9.5 min; 5 % B at t = 12 min]. Metabolites (1 μL injection volume per sample) were separated at 40 °C using a Waters BEH-C18 (100 × 2.1 mm; 1.7 μm Particle size) column. MRM transitions for M8OI, HO8IM and COOH7IM were 195.2 → 83.1, 211.2 → 83.1 and 225.2 → 83.1 respectively, with a collision energy of 20eV.

2.10. CYP450 PPXE activity assay

A kit purchased from Promega (UK) was used to examine Luciferin-PPXE metabolism, using a luminometer to monitor liberated luciferin. This activity is DMSO tolerant and recommended for determining CYP3A4 activities. Activities were determined in cell extracts or supernatants diluted in 100 mM potassium phosphate buffer pH 7.5 at 25 °C with 25 μM PPXE substrate and initiated through the addition of 1 mM NADPH. Replicates performed in the absence of cell/supernatant extracts and separately in the absence of NADPH were also included.

2.11. Seahorse analyses

Mitochondrial activities - oxygen consumption rate (OCR) and extracellular acidification rate (ECAR) - as indicators of mitochondrial respiration and glycolysis, were assessed using the Seahorse XF analyser XFe96 (Agilent, Santa Clara, US) essentially following the manufacturer's guidelines with analysis using Seahorse Wave software 2.6.0. Calibration cartridges were hydrated for 24 h prior to experiments using the Seahorse XF Calibrant at 37 °C at ambient air CO₂ levels. Cells were cultured in seahorse XF cell culture microplates (96 wells). Prior to any measurements, their standard growth culture media were discarded and cells washed twice with assay medium (freshly prepared 5.5 mM glucose, 1 mM pyruvate, 2 mM glutamine in Seahorse XF Base Medium, pH 7.4). Assays were performed in 180 μL assay medium/well after incubation at 37 °C at ambient air CO₂ levels for 1 h.

OCR and ECAR values were normalised to protein content in each well at the end of the experiment, using the Bradford reagent (Sigma, Poole, UK).

2.12. Data Handling and Statistics

Data are expressed as means ± standard deviation (SD). Comparisons between means were carried out using the Student's T test for 2 group comparisons and one way analysis of variance (ANOVA) test for multiple group comparisons, followed by a Tukey's post hoc test. For all statistical tests, the level of significance was fixed at $p < 0.05$. GraphPad Prism® software package, version 8 (GraphPad Software Inc., USA) was used to carry out all statistical tests and for calculating LC50% values.

3. Results

3.1. u-HepaRG cells are relatively insensitive to the toxic effects of M8OI

The toxicity of M8OI was examined in u-HepaRG cells and compared to B-13 cells using MTT reduction as a proxy for viability. Previous work has confirmed that M8OI and its metabolites do not directly inhibit MTT reduction (Hedya et al., 2023). Fig. 1c demonstrates that M8OI was toxic to B-13 cells in a dose-responsive manner similar to that previously reported (Abdelghany et al., 2020). In comparison, u-HepaRG cells were in excess of 20-fold less sensitive to M8OI when treated in their recommended culture medium (WME). WME contains higher levels of glucose (11 mM) whereas the B-13 medium contains normal glucose levels (5 mM). Since additional glucose has been shown to afford some protection from M8OI in B-13 cells (Probert et al., 2018), the effect of treating u-HepaRG cells in DMEM (containing 5 mM lower glucose) was examined. Fig. 1c demonstrates that transferring HepaRG cells to the medium did not markedly increase u-HepaRG cell sensitivity to M8OI.

Fig. 1d–g indicate that despite showing less sensitivity to M8OI than B-13 cells, u-HepaRG cells nonetheless initially underwent an apoptotic mode of cell death based on statistically significant increases in surface exposed phosphatidylserine (Fig. 1d) and caspase 3/7 activity (Fig. 1e) in the absence of a loss of membrane integrity based on lactate dehydrogenase (LDH) leakage (Fig. 1f) and trypan blue exclusion (Fig. 1g). At very high concentrations (1 mM M8OI) there was evidence of necrosis, likely related to an eventual collapse of apoptosis to necrosis. These characteristics of cell death were also observed with gliotoxin (an inducer of apoptosis) and contrasts with chlorpromazine, which induces a necrotic mode of cell death (Wright et al., 2001; Orr et al., 2004).

Fig. 1h confirms that apoptosis forms a component of cell death in response to M8OI, since there was a cleavage of DNA to a nucleosomal ladder, a process considered diagnostic of programmed cell death (Compton, 1992; Kari et al., 2022).

3.2. CYP3A7-mediated metabolism partially protects u-HepaRG cells from the toxic effects of M8OI

Previous work with human hepatocytes (Probert et al., 2018), differentiated HepaRG cultures (Leitch et al., 2021) and mice (Young et al., 2020) have demonstrated that M8OI is monooxygenated on the alkyl omega carbon to HO8IM followed by oxidation to its carboxylic acid (COOH7IM) (Fig. 2a). No other metabolite has been detected.

In human hepatocyte systems, metabolism is inhibited by the CYP3A inhibitor ketoconazole (Leitch et al., 2021). More recently, the major expressed human CYP3A4 has definitively been shown to mediate the monooxygenation of M8OI to HO8IM (Leitch et al., submitted).

Fig. 2b demonstrates that in our hands, u-HepaRG cells did not express detectable levels of the major-expressed adult hepatic CYP3A4. CYP3A5 was also not detected. In contrast, the human fetal liver form - CYP3A7 - was determined to be present in u-HepaRG cells. We therefore hypothesised that the resistance of u-HepaRG cells to the toxic effects of M8OI was associated with a CYP3A7-dependent oxidation of M8OI to HO8IM followed by potentially further oxidation to the COOH7IM metabolite.

Fig. 2c and d confirm that M8OI was removed from the medium of u-HepaRG cultures with an approximate half-life of around 6 h and a time-dependent increase in the concentration of HO8IM and COOH7IM metabolites. This contrasts with B-13 cells, which do not show any metabolism of M8OI (Hedya et al., 2023). Addition of ketoconazole blocked the disappearance of M8OI and appearance of both metabolites, supporting a major role for CYP3A7 in the metabolism of M8OI in u-HepaRG cells. Fig. 2e indicates that HO8IM and COOH7IM were less toxic to u-HepaRG cells (by a factor of at least 100 fold). Metabolism of M8OI by u-HepaRG cells therefore represents a detoxification pathway for M8OI in u-HepaRG cells.

We therefore further hypothesised that addition of ketoconazole to HepaRG cells should lead to an increase in sensitivity to M8OI through its ability to block CYP3A7-mediated metabolism to less toxic metabolites. Fig. 2e demonstrates that ketoconazole increased u-HepaRG cell sensitivity to M8OI, supporting a protective role for CYP3A7. However, protection was limited to at most 20%, suggesting that an additional factor(s) is responsible for u-HepaRG cell resistance to M8OI.

3.3. Ketoconazole exacerbates the toxicity of M8OI through its inhibition of CYP3A7

The probe substrate PPXE (for CYP3A isoforms) was employed to determine whether u-HepaRG cells express functional CYP3A activities. Fig. 3a indicates that u-HepaRG cells expressed low levels of activity compared to several human hepatocyte extracts. In contrast, the human breast cancer MCF7 cell line did not express any detectable PPXE activity. Examination of PPXE activities in supersomes, which contain a single CYP isoform in addition to the CYP reductase required for activity confirms that CYP3A4, CYP3A5 and CYP3A7 are similarly active against the PPXE substrate. In contrast, CYP2A6 showed negligible activity toward this substrate in that apparent activity was similar to supersome preparations incubated in the absence of NADPH and barely above no enzyme controls. Of note, CYP3A supersomes containing additionally cytochrome b5 showed marked (>20 fold) increases in PPXE activity, in contrast to CYP2A6.

Ketoconazole dose-dependently inhibited PPXE metabolism in supersomes containing CYP3A4, CYP3A5 or CYP3A7 (Fig. 3c). A comparison with u-HepaRG cell extract activities suggests that ketoconazole inhibition most closely resembles an inhibition of CYP3A7 rather than CYP3A4 or CYP3A5. The dose-response inhibition of PPXE activity by ketoconazole was also mirrored by a similar dose-responsive increase in M8OI toxicity with ketoconazole (Fig. 3d).

These data therefore suggest that u-HepaRG cells express functional PPXE activity mediated primarily via CYP3A7. Inhibition of CYP3A7 with ketoconazole resulted in a potentiation of M8OI toxicity. However,

there was a limit to the ability of ketoconazole to increase toxicity, suggesting that CYP3A7-mediated metabolism of M8OI in u-HepaRG cells was only a contributor to the relative insensitivity of u-HepaRG cells to M8OI, when compared to B-13 cells.

3.4. u-HepaRG cells have a lower oxygen consumption rate (OCR), a reduced reliance on mitochondrial activity compared to B-13 cells

In B-13 cells, M8OI targets mitochondrial electron transport leading to an inhibition in both oxygen consumption and mitochondrial ATP generation (Abdelghany et al., 2020). B-13 cells are able to compensate to some extent through an increase in glycolytic flux in combination with the generation of lactate as the final product. Increasing the medium glucose concentration therefore protects against M8OI toxicity in B-13 cells through a compensatory increase in lactate production, whereas this protection is lost when glucose is replaced with galactose (Abdelghany et al., 2020; Probert et al., 2018).

Fig. 4a confirms the protective role of glucose - and lack of protection by galactose - in B-13 cells exposed to M8OI. In contrast, glucose failed to protect u-HepaRG cells from M8OI toxicity (Fig. 4b). Interestingly, replacing glucose with galactose induced a very mild degree of protection from M8OI in u-HepaRG cells. The mild protective effect is dose-dependent, but only statistically significantly higher than M8OI alone in the 20–30 mM range. Circumventing the Crabtree effect (i.e. through glucose replacement with galactose) increases mitochondrial carbon oxidation via the TCA cycle with concomitant increased oxidative phosphorylation (Marroquin et al., 2007; Dykens et al., 2008). The mild protective effect of galactose in u-HepaRG cells may be associated with a mild increase in resilience of cells to cellular stress when mitochondria are more active in cells.

Comparing the growth and metabolic characteristics of B-13 and u-HepaRG cells (Table 1) demonstrates that they have similar doubling times (and therefore likely similar energetic requirements under their respective standard culture conditions), yet markedly divergent consumption rates for glucose. Further, u-HepaRG cells consume low levels of oxygen compared to B-13 cells. Although u-HepaRG cells generate more lactate per unit glucose consumed, based on acidification of the medium, it is likely that glycolytic flux to lactate is not a major oxidative pathway in u-HepaRG cells.

Given that the key initiating event in M8OI toxicity is an inhibition of oxidative phosphorylation, a contribution to the resistance of u-HepaRG to M8OI toxicity is likely associated with u-HepaRG's reduced reliance on mitochondrial activity. To test this hypothesis, the effect of M8OI on u-HepaRG viability was compared in glucose or galactose containing medium. Fig. 4c and d demonstrate that exposing u-HepaRG cells to M8OI in glucose- and galactose-free medium significantly enhances the toxicity of M8OI indicating the cells were significantly sensitized through energetic restriction. In galactose containing medium, u-HepaRG cells showed a marked increase in sensitivity compared to medium containing glucose and a sensitivity approaching that seen with B-13 cells.

A similar qualitative profile of oxygen consumption changes in response to classic electron transport chain inhibitors - oligomycin, FCCP and rotenone/antimycin A - was observed in B-13 and u-HepaRG cells (Fig. 4e). However, M8OI was less potent in its inhibition of oxygen consumption rate in u-HepaRG cells compared to B-13 cells (Fig. 4f), suggesting that the affinity of M8OI for its unknown mitochondrial molecular target is also lower in human (u-HepaRG cells) versus rat (B-13 cells).

4. Discussion

This study examines for the first time, the effects of M8OI exposure on u-HepaRG cells. The data demonstrate that u-HepaRG cells under standard culture conditions are relatively insensitive to M8OI with regard to cell death, when compared to B-13 cells. Furthermore, the

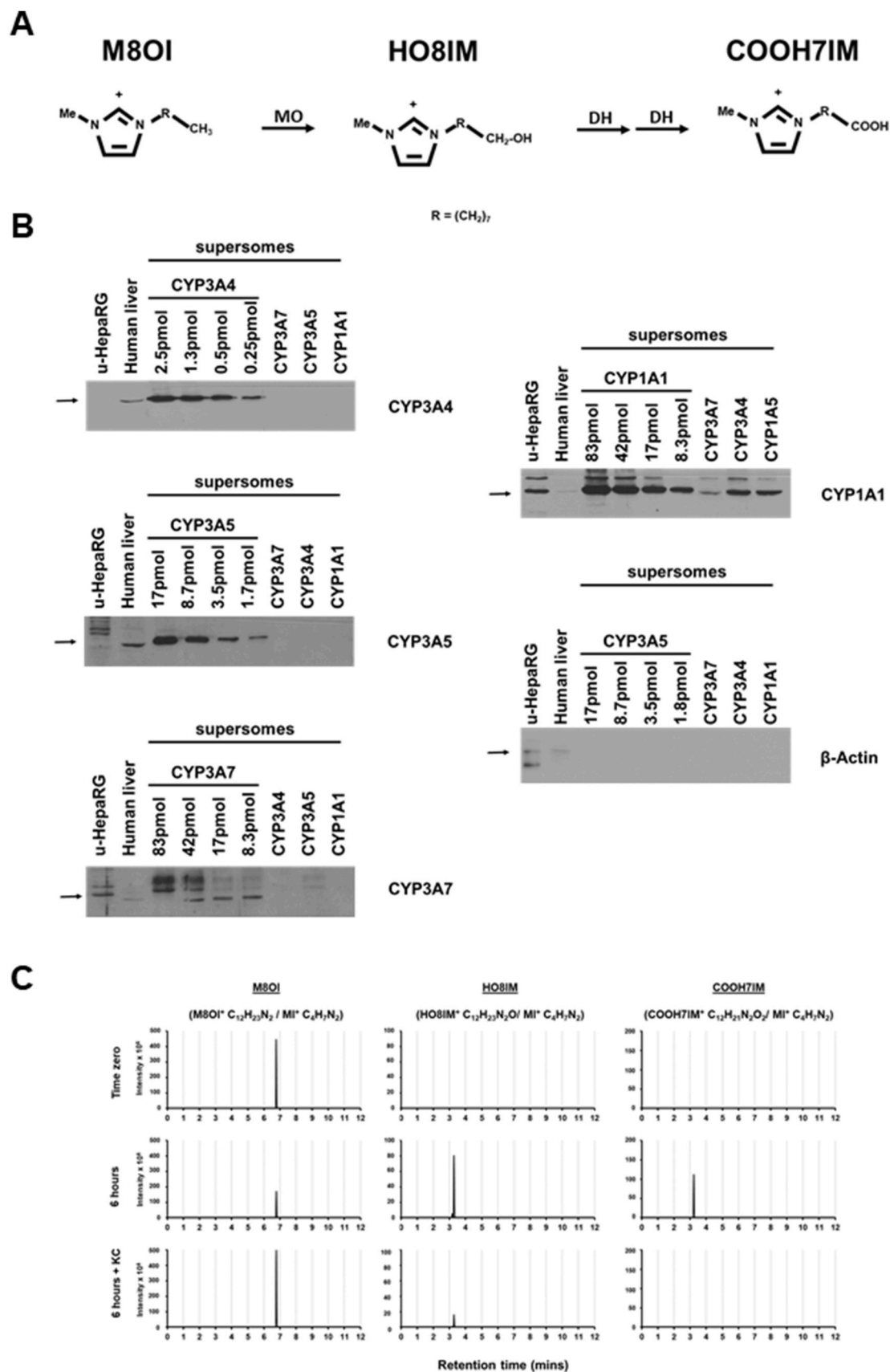


Fig. 2. u-HepaRG cells metabolise M8OI to less-toxic metabolites. **A**, schematic diagram of the known metabolic pathway for M8OI based on work in human and rodent hepatocyte and rodent work in vivo. MO, monooxygenase(s); DH, dehydrogenase(s). **B**, Western blots for the indicated target protein. u-HepaRG, 20 µg protein/lane; human liver extract prepared from freshly hepatocytes (NHL6) isolated and archived from a previous study (Leitch et al., 2021), 20 µg protein/lane. Note, for supersome controls, the highest concentration used using the correct antibody was employed (i.e. 83pmoles CYP1A1; 2.5pmoles CYP3A4; 17pmoles

CYP3A5 and 83pmoles CYP3A7). C, Typical LC/MS chromatographs for M8OI and its known metabolites – HO8IM and COOH7IM - using a combination of the intact parent ion and the fragment methylimidazolium fragment ion (MI^+). Data typical of 3 separate experiments; KC, metabolism examined in the presence of 10 μ M ketoconazole. D, Timecourse for changes in concentrations of M8OI and metabolites in control STIM medium (left panel) or STIM medium supplemented with 10 μ M ketoconazole. Data are the mean and SD of 3 separate experiments. E, Effects of M8OI, HO8IM or COOH7IM on the viability of u-HepaRG cells based on MTT reduction after 24 h. Data are the mean and SD of 4 separate determinations, typical of at least 3 separate experiments. $LC_{50\%}$ for M8OI, $290 \pm 75 \mu$ M; for HO8IM, > 5 mM and for COOH7IM, > 5 mM *Statistically significantly different (two tailed) from control vehicle using one way ANOVA, followed by a Tukey's post hoc test ($p < 0.05$).

concentrations required to induce u-HepaRG cell death are far in excess of the levels relevant to the general population and potential exposure via the limited data available regarding environmental contamination (highest soil levels 0.3 ppm (Leitch et al., 2020a)). However, the data indicate that an apoptotic mode of cell death occurs in u-HepaRG cells treated with M8OI.

The mechanisms underlying B-13 cell sensitivity were examined recently. Neither B-13, nor B-13/H cells appreciably metabolise M8OI indicating that metabolism does not play a role in their divergent sensitivity to M8OI (Hedya et al., 2023). However, B-13/H cells have higher expression levels of p-glycoprotein than B-13 cells and p-glycoprotein substrates/inhibitors sensitize B-13 cells to M8OI (Hedya et al., 2023). A significant driver for B-13 sensitivity therefore appears to be associated with reduced capability to excrete M8OI from the cell. However, p-glycoprotein inhibition did not significantly affect M8OI toxicity in u-HepaRG cells (data not included), suggesting that M8OI excretion by p-glycoprotein is not a significant determinant in M8OI toxicity in u-HepaRG cells.

Previous work with HepaRG cells differentiated into hepatocytes and cholangiocytes has shown that M8OI is monooxygenated by a ketoconazole-inhibited cytochrome P450(s). This step is likely primarily mediated in differentiated HepaRG cells by the adult human hepatic CYP3A4 form, with a potential contribution from CYP3A5, since these forms were most active in a screen for HO8IM production with a range of human CYPs (supersome preparations) (Leitch et al., 2024). In differentiated HepaRG cells, HO8IM is then oxidized by alcohol and acetaldehyde dehydrogenase(s) to finally form the carboxylic acid metabolite COOH7IM (Leitch et al., 2021). Little further metabolic change occurs from this point, including any action by phase 2 enzymes.

Based on previous (Probert et al., 2018; Leitch et al., 2021) and the present LC-MS/MS data, a methylimidazolium moiety fragment (m/z 83) is observed, not a fragment commensurate with oxidation on the methyl group present in M8OI. Further, oxidative metabolites of M8OI have identical retention times to authentic HO8IM and COOH7IM metabolites. To date, all data indicate oxidation of M8OI on the 8C alkyl chain rather than the methyl group. This is in alignment with microbial M8OI degradation data using sewage sludge, a system containing a vast range of microbial species and metabolic options. In these systems, oxidation of M8OI is restricted to oxidation on the 8C chain, with no activity seen on the methyl group (Markiewicz et al., 2015).

The current study shows that M8OI is metabolised qualitatively similarly in u-HepaRG cells to human hepatocytes. However, uHepaRG cells did not express detectable levels of CYP3A4 and CYP3A5 proteins, rather they expressed the fetal hepatic isoform CYP3A7. Some elegant work by Tsuji et al. (2014) created transgenic HepaRG cells by replacing the protein-coding regions of human CYP3A4 and CYP3A7 with enhanced green fluorescent protein and DsRed reporters, respectively (in a bacterial artificial chromosome vector that included whole regulatory elements). They demonstrated that the intensity of DsRed fluorescence was initially high during the proliferation of transgenic HepaRG cells (i.e. equivalent to u-HepaRG cells) and that most EGFP-positive cells were derived from those in which DsRed fluorescence was extinguished. CYP3A7 mRNA was also detected in u-HepaRG cells but also persisted in differentiated HepaRG cells. The work of Tsuji et al. (2014) work supports our conclusion that CYP3A7 is expressed in u-HepaRG cells.

Since the M8OI metabolites are less toxic, co-treating u-HepaRG cells with ketoconazole would be expected to increase their sensitivity to

M8OI. Although ketoconazole was able to effectively block M8OI metabolism by u-HepaRG cell, it only produced a limited enhancement in M8OI toxicity. The concentration of ketoconazole required to produce this effect also mirrored its ability to inhibit CYP3A7 rather than the more sensitive CYP3A5 and CYP3A4 forms, supporting a prominent role for CYP3A7 in u-HepaRG-mediated M8OI metabolism.

Given that ketoconazole had limited effects on M8OI toxicity in u-HepaRG cells, additional differences between B-13 and u-HepaRG cells were considered. The mode of action of M8OI appears to be similar in the cell types examined thus far, and involves a block in mitochondrial oxidative phosphorylation, likely through interactions upstream of complex III (Abdelghany et al., 2020). The inhibition in oxidative phosphorylation leads to an increase in medium glucose consumption and lactate production in B-13 cells, suggestive of a compensatory increase in glycolysis (Abdelghany et al., 2020). Accordingly, provision of additional glucose to B-13 cells treated with M8OI was effective in ameliorating M8OI toxicity (Probert et al., 2018). Increasing the concentration of glucose had no effect in protecting u-HepaRG cells from M8OI toxicity, in contrast to B-13 cells.

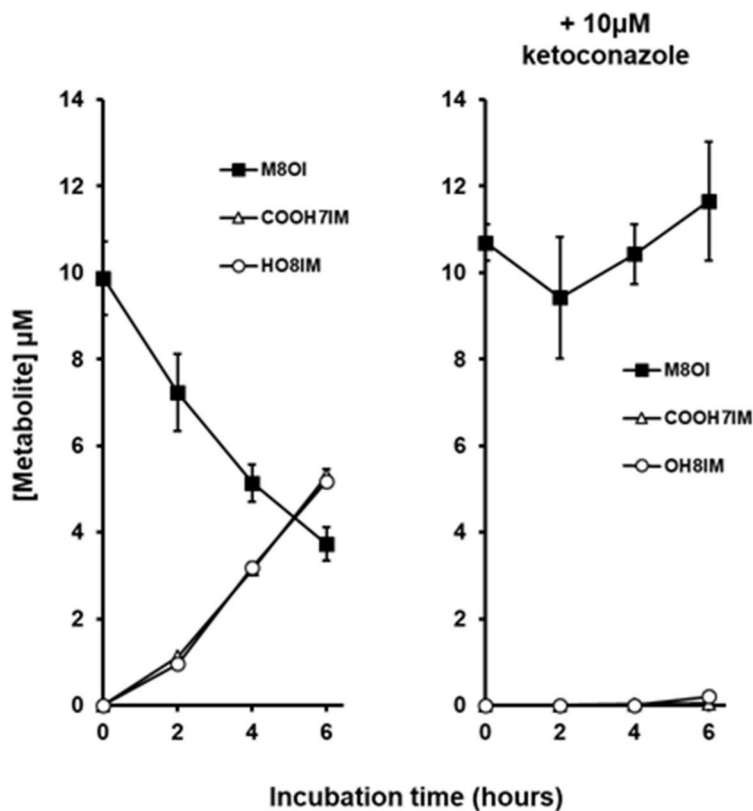
The ‘‘Crabtree effect’’ is a phenomenon that refers to the adaptation of cultured cells in glucose-containing medium to a glycolytic phenotype and away from oxidative phosphorylation (de Kok et al., 2021). u-HepaRG cells used significantly less oxygen than B-13 cells when normalised for total cell protein and replacing glucose with galactose, sensitized u-HepaRG cells such that they showed a similar sensitivity to M8OI as B-13 cells. These observations suggest that u-HepaRG cells have adapted and reduced their reliance on oxidative phosphorylation under normal propagation. Accordingly, in addition to a reduced sensitivity to M8OI inhibition in u-HepaRG cells compared to B-13 cells, the impact of a mitochondrial toxin targeting mitochondrial oxidative phosphorylation is likely to be significantly reduced due to the Crabtree effect, as noted previously by others in HepG2 cells (Marroquin et al., 2007; Dykens et al., 2008). However, it is unclear why increasing medium glucose concentrations does not protect u-HepaRG cells from M8OI. It may suggest a limited ability of the cells to produce increased lactate from pyruvate in response to M8OI. It may also suggest that u-HepaRG cells rely heavily on carbon sources other than glucose.

It has been proposed that M8OI could be a hazard with respect to triggering PBC because the COOH7IM metabolite is amenable to enzymatic conjugation to PDC-E2 in place of lipoic acid in a cell-free system (Probert et al., 2018; Leitch et al., 2020). However, this alone is unlikely to be the only process required to trigger a loss of tolerance to PDC-E2 and other lipoylated proteins in vivo. Apoptosis and presentation of non-glutathionylated PDC-E2 is also required. In this respect, M8OI induces apoptosis in a variety of cell types (Jing et al., 2013; Li et al., 2015; Ma and Li, 2018) and this is accompanied by an increase in oxidative stress, the latter likely to contribute to oxidation of reduced glutathione.

Thus, the u-HepaRG platform provides a human liver cell system that could be used to study how a xenobiotic could produce all the adverse pathways required in the initiation of PBC. In contrast, B-13 cells lack the ability to metabolise M8OI to COOH7IM and therefore lack one of the critical key pathways.

Given the current aspiration to reduce animal use in toxicological investigations and biological research more widely, cognisance of the metabolic adaptations apparent in cell lines may be critical for their successful application, particularly in regulatory decisions. It is likely cell-based in vitro studies will form a significant component of NAMs and translating in vitro observations to toxicological implication with a

D



E

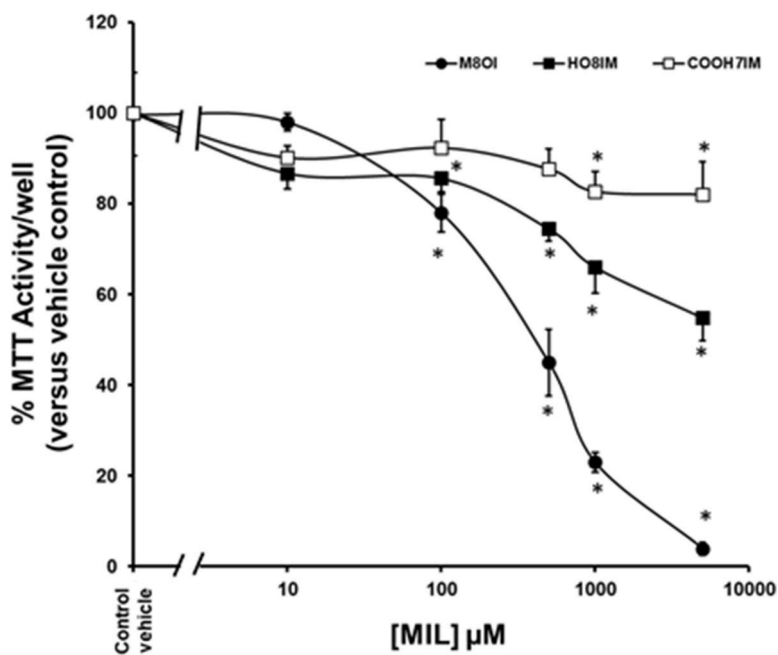


Fig. 2. (continued).

reasonable degree of quantitative certainty will be challenging.

CRediT authorship contribution statement

Tarek M. Abdelghany: Writing – review & editing, Visualization,

Methodology, Investigation, Formal analysis, Data curation. **Shireen A. Hedy**: Writing – review & editing, Visualization, Investigation, Data curation. **Alex Charlton**: Writing – review & editing, Validation, Methodology, Investigation. **Fahad A. Aljehani**: Writing – review & editing, Investigation. **Khalid Alanazi**: Investigation. **Alaa A.**

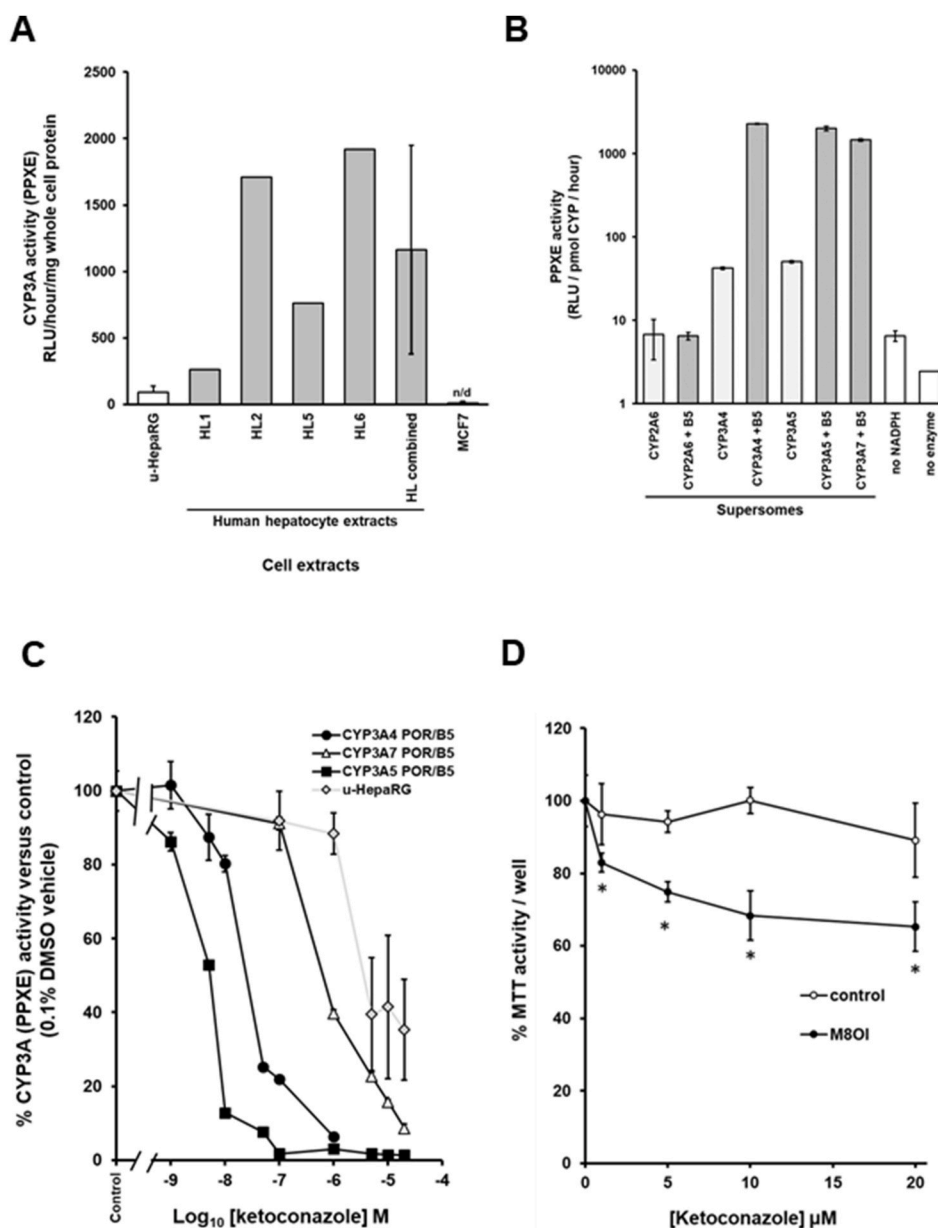


Fig. 3. Ketoconazole-dependent CYP3A activity and its effects on M8OI toxicity. **A**, Comparing the CYP3A (PPXE) enzyme activity in u-HepaRG, human hepatocytes and MCF7 cells. All data are the mean and SD of at least 3 separate experiments except for human liver (HL) samples, which is a mean of 4 determinations from the same extract. HL combined represents a mean and SD of the 4 separate HL activities. **B**, PPXE activities in the indicated supersome preparations. All preparations include expression of CYP-reductase (white bars) or as indicated, additionally cytochrome B5 (B%, grey bars). Note, CYP3A7 supersomes are only available with additional cytochrome B5. Data are the mean and SD of 4 determinations. No NADPH, assay performed with CYP3A5 supersomes in the absence of NADPH; no enzyme, assay performed in the absence of supersomes. **C**, Effect of ketoconazole on CYP3A (PPXE) activity mediated by the indicated supersome prep. Data are the mean and SD of 4 separate determinations from the same experiment, typical of at least 5 separate experiments. **D**, Effects of ketoconazole on the toxicity of 250 μM M8OI based on MTT reduction after 24 h. Data are the mean and SD of 4 separate determinations, typical of at least 4 separate experiments. *Statistically significantly different (two tailed) from control (no ketoconazole) using one way ANOVA, followed by a Tukey's post hoc test ($p < 0.05$).

Budastour: Writing – review & editing, Investigation. **Larissa Marin:** Investigation. **Matthew C. Wright:** Writing – original draft, Validation, Supervision, Resources, Project administration, Methodology, Investigation, Funding acquisition, Conceptualization.

Declaration of competing interest

The authors declare the following financial interests/personal relationships which may be considered as potential competing interests: Shireen Hedy reports financial support was provided by Newton-Mosharafa Fund. Fahad Aljehani reports financial support was

provided by Royal Government of Saudi Arabia. The authors declare that funding has been received in the past (2019) to investigate the metabolism of 3 compounds for Lubrizol (Wright). None of the compounds were ionic liquids and this work is considered by the authors to be unrelated to the study described herein. Wright has served as an Expert Member of the scientific panel on Food Additives and Nutrient Sources (ANS) of the European Food Safety Authority (2011–2018); is currently an expert Member of the scientific panel on Food Additives and Flavourings (FAF) of the of the European Food Safety Authority (2020 – present); is currently a member of the UK Committee on Toxicity (2017-present) and is currently a member of the UK Expert Committee

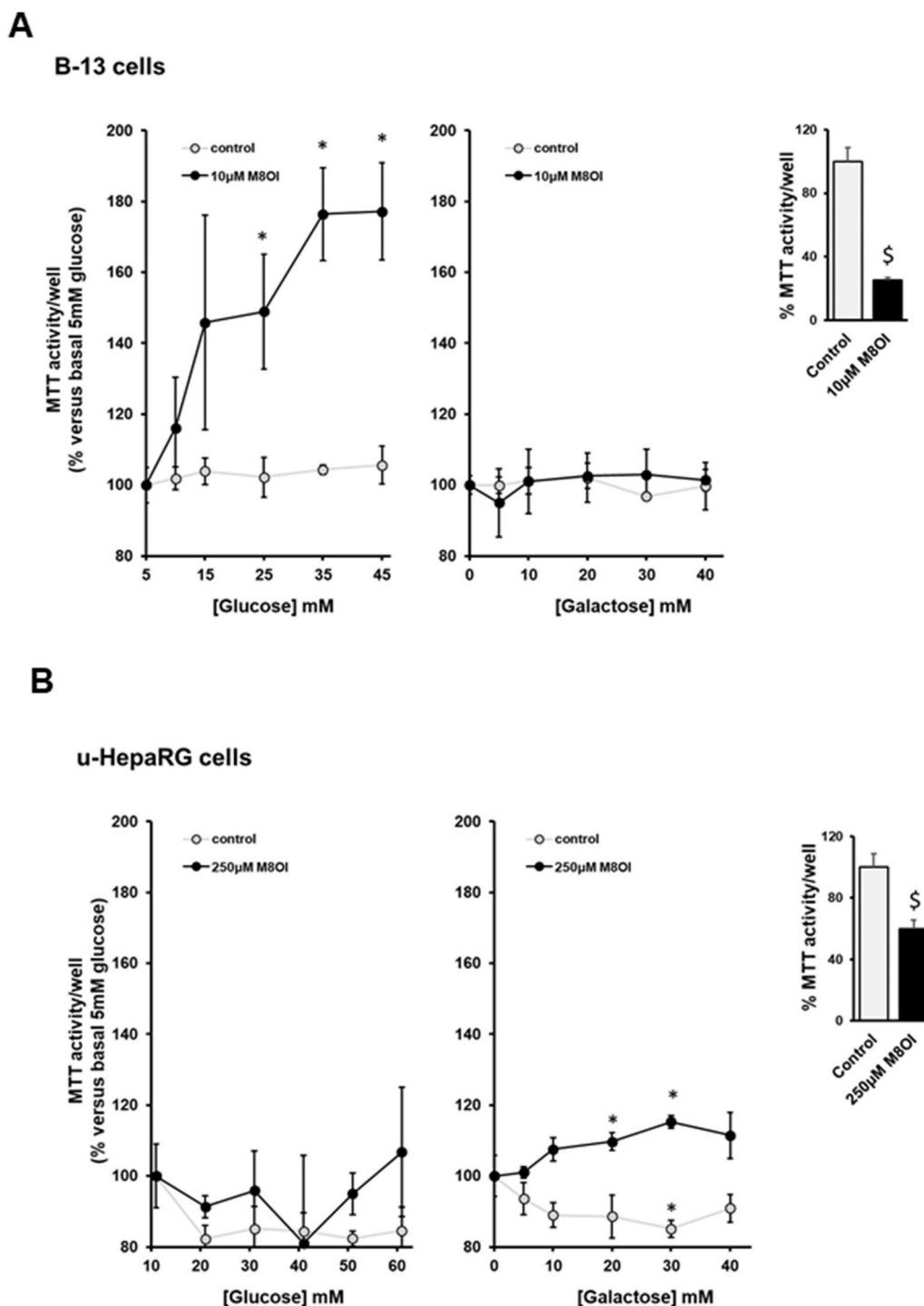
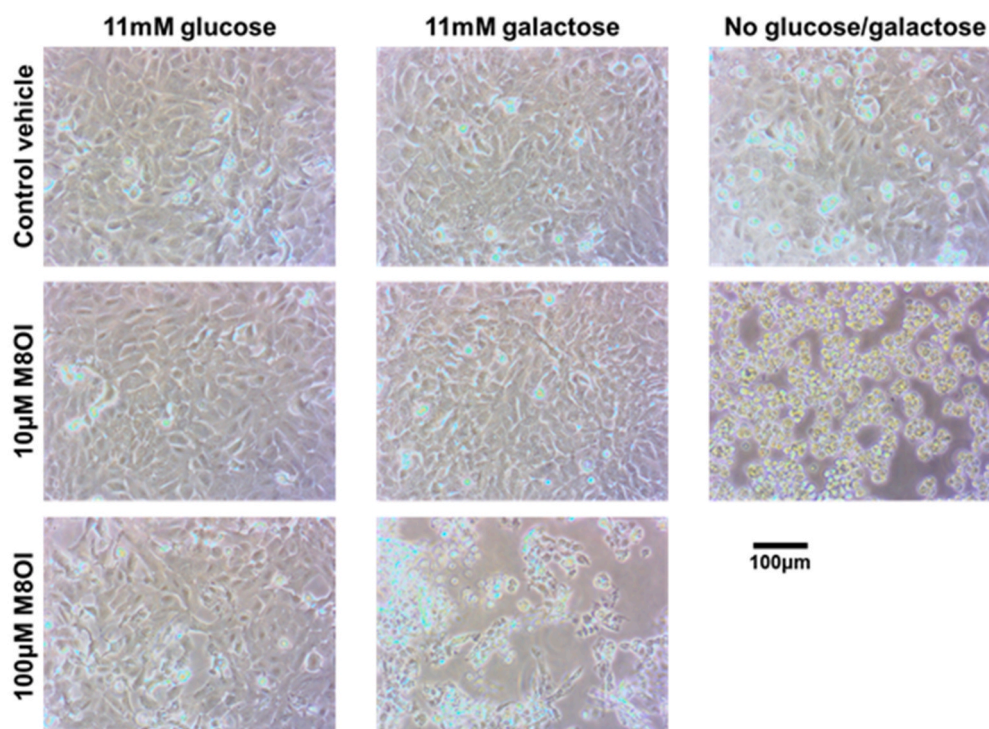


Fig. 4. u-HepaRG and B-13 cells show divergent responses to protection from glucose and galactose. **A**, Effects of additional glucose (main left panel) or galactose (main right panel) on the viability of B-13 cells treated with 10 μ M M8OI, based on MTT reduction after 24 h. Far right panel, comparison of % MTT activity in untreated versus 10 μ M M8OI treated cells in control media (i.e. 5 mM glucose containing media). Data are the mean and SD of 4 separate determinations, typical of at least 8 separate experiments. Statistically significantly different (two tailed) from no addition glucose or galactose using one way ANOVA*, followed by a Tukey's post hoc test or from control using the Student's T test^s for 2 group comparisons ($p < 0.05$). **B**, Effects of additional glucose (main left panel) or galactose (main right panel) on the viability of u-HepaRG cells treated with 250 μ M M8OI, based on MTT reduction after 24 h. Far right panel, comparison of % MTT activity in untreated versus 250 μ M M8OI treated cells in control media (i.e. 11 mM glucose containing media). Data are the mean and SD of 4 separate determinations, typical of at least 3 separate experiments. Statistically significantly different (two tailed) from no addition glucose or galactose using one way ANOVA*, followed by a Tukey's post hoc test or from control using the Student's T test^s for 2 group comparisons ($p < 0.05$). **C**, Photomicrographs of u-HepaRG cells treated as indicated for 24 h. Data typical of at least 4 separate experiments. **D**, M8OI dose-response toxicity in u-HepaRG cells treated in WME in the absence of glucose in standard culture (no sugars), standard culture with glucose (11 mM glucose) or with galactose instead of glucose (11 mM galactose). Viability based on % MTT reduction after 24 h treatment with M8OI. LC_{50%} for M8OI in presence of no sugars, $3 \pm 1.8 \mu$ M; in presence of galactose, $12 \pm 8.5 \mu$ M and in the presence of glucose $370 \pm 62 \mu$ M. Far right panel, comparison of MTT activity in each medium after 24 h, in the absence of M8OI. Data are the mean and SD of 4 separate determinations, typical of at least 3 separate experiments. **E**, OCR in B-13 and u-HepaRG cells performed at the same time and under the same conditions, with data normalised to total cell protein post analysis. Data are the mean and SD of 6 separate determinations from the same experiment, typical of at least 3 separate experiments. Arrows indicate addition of

various standard modulators of mitochondrial function: Olmicin, addition of 1 μM oligomycin; FCCP, addition of 1 μM of FCCP (carbonyl cyanide 4-(trifluoromethoxy)phenylhydrazone) and Rnone/AA, addition of 0.5 μM rotenone/0.5 μM antimycin A. F, OCR in u-HepaRG cells and B-13 cells treated with M8OI expressed relative to their respective OCR prior to addition of M8OI. Data are the mean and SD of 6 separate determinations from the same experiment, typical of 3 separate experiments. Statistically significantly different (two tailed) from B-13 cells using the Student's T test⁵ for 2 group comparisons ($p < 0.05$).

C



D

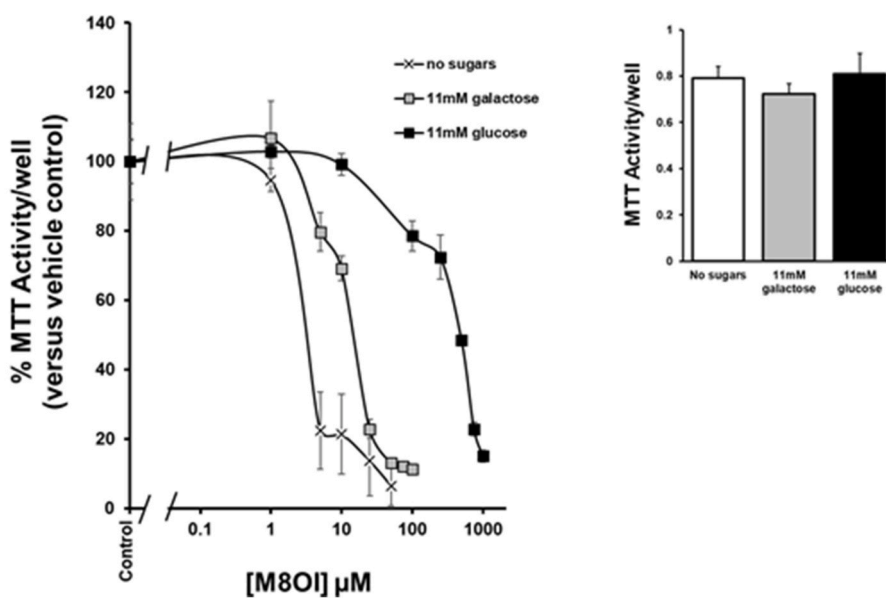


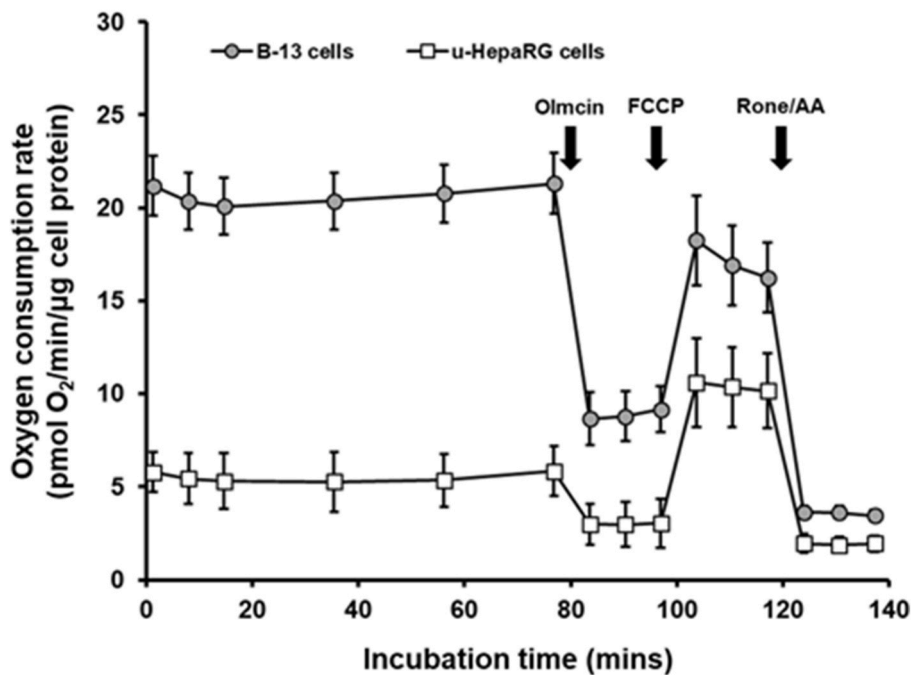
Fig. 4. (continued).

for Pesticides (2022- present). The authors certify that their freedom to design, conduct, interpret, and publish research was - and is not - compromised by any controlling sponsor. The other authors declare they

have no actual or potential competing financial interests.

If there are other authors, they declare that they have no known competing financial interests or personal relationships that could have

E



F

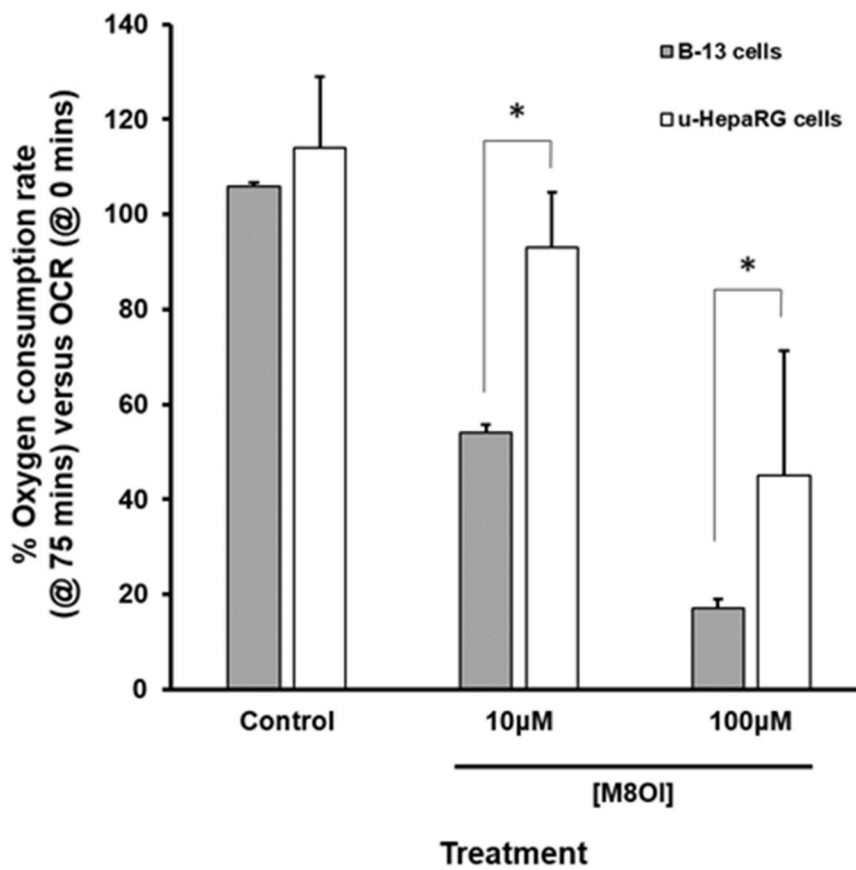


Fig. 4. (continued).

Table 1
Growth and selected metabolic characteristic of B-13 and u-HepaRG cells.

	B-13s	u-HepaRGs
Proliferation (doubling time in hr)	30 ± 7.3*	29 ± 6.2
Medium glucose consumption (μmol/hr/mg protein)	0.72 ± 0.024 [§]	0.17 ± 0.023
Medium lactate production (μmol/hr/mg protein)	1.7 ± 0.12 [§]	0.54 ± 0.104
medium lactate produced/medium glucose produced	2.4	3.2
O ₂ consumption (pmol/min/mg protein)	19 ± 1.6	5.3 ± 0.11
ECAR (mpHunits/min/μprotein)	6.1 ± 0.36	2.2 ± 0.42

Proliferation, glucose consumption and lactate production were determined in the standard growth medium used for these cells and in which toxicity studies with M8OI were performed. Data are the mean and SD of 3 separate experiments. Oxygen consumption was determined using a seahorse machine and in a medium modified for these studies. Taken from Probert et al. (2014)* and Abdelghany et al. (2020)[§]

appeared to influence the work reported in this paper.

Data availability

Data will be made available on request.

Acknowledgements

This work was funded by the Newton-Mosharafa Fund (in the form of a studentship supporting S.A.H.), the Royal Government of Saudi Arabia (in the form of a studentship supporting F.A.A) and the Embassy of the state of Kuwait (in the form of a studentship supporting A.A.B.).

References

Ala, A., Stanca, C.M., Bu-Ghanim, M., Ahmado, I., Branch, A.D., Schiano, T.D., Odin, J. A., Bach, N., 2006. Increased prevalence of primary biliary cirrhosis near Superfund toxic waste sites. *Hepatology* 43, 525–531.

Aninat, C., Piton, A., Glaise, D., Le Charpentier, T., Langouët, S., Morel, F., Guguen-Guillouzo, C., Guillouzo, A., 2006. Expression of cytochromes P450, conjugating enzymes and nuclear receptors in human hepatoma HepaRG cells. *Drug Metab. Dispos.* 34, 75–83.

Arsenijevic, A., Milovanovic, M., Milovanovic, J., Stojanovic, B., Zdravkovic, N., Leung, P.S., Liu, F.T., Gershwil, M.E., Lukic, M.L., 2016. Deletion of galectin-3 enhances xenobiotic induced murine primary biliary cholangitis by facilitating apoptosis of BECs and release of autoantigens. *Sci. Rep.* 6, 23348.

Compton, M.M., 1992. A biochemical hallmark of apoptosis: internucleosomal degradation of the genome. *Cancer Metastasis Rev.* 11, 105–119.

de Kok, M.J.C., Schaapherder, A.F., Wüst, R.C.I., Zuiderwijk, M., Bakker, J.A., Lindeman, J.H.N., Le Dévédec, S.E., 2021. Circumventing the Crabtree effect in cell culture: a systematic review. *Mitochondrion* 59, 83–95.

Deyab, M.A., Mohsen, Q., 2021. Improving the sustainability of biodiesel by using imidazolium-based ionic liquid. *Sci. Rep.* 11, 16832.

Dykens, J.A., Jamieson, J., Marroquin, L., Nadanaciva, S., Billis, P.A., Will, Y., 2008. Biguanide-induced mitochondrial dysfunction yields increased lactate production and cytotoxicity of aerobically-poised HepG2 cells and human hepatocytes in vitro. *Toxicol. Appl. Pharmacol.* 233, 203–210.

Hedya, S., Charlton, A., Leitch, A.C., Aljehani, F.A., Pinker, B., Wright, M.C., Abdelghany, T.M., 2023. The methylimidazolium ionic liquid M8OI is a substrate for OCT1 and p-glycoprotein-1 in rat. *Toxicol. Vitro* 88, 105550.

Hirschfield, G.M., Dyson, J.K., Alexander, G.J.M., Chapman, M.H., Collier, J., Hübscher, S., Patanwala, I., Pereira, S.P., Thain, C., Thorburn, D., Tiniakos, D., Walmsley, M., Webster, G., Jones, D.E.J., 2018. The British Society of Gastroenterology/UK-PBC primary biliary cholangitis treatment and management guidelines. *Gut* 67, 1568–1594.

Jing, C., Li, X., Zhang, J., Wang, J., 2013. Responses of the antioxidant system in QGY-7701 cells to the cytotoxicity and apoptosis induced by 1-octyl-3-methylimidazolium chloride. *J. Biochem. Mol. Toxicol.* 27, 330–336.

Kari, S., Subramanian, K., Altomonte, I.A., Murugesan, A., Yli-Harja, O., Kandhavelu, M., 2022. Programmed cell death detection methods: a systematic review and a categorical comparison. *Apoptosis* 27, 482–508.

Leitch, A.C., Lakey, A.F., Hotham, W.E., Agius, L., Kass, G.E.N., Blain, P.G., Wright, M.C., 2018. The ionic liquid 1-octyl-3-methylimidazolium M8OI is an activator of the human estrogen receptor alpha. *Biochem. Biophys. Res. Commun.* 503, 2167–2172.

Leitch, A.C., Abdelghany, T.M., Probert, P.M., Dunn, M.P., Meyer, S.K., Palmer, J.M., Cooke, M.P., Blake, L.I., Morse, K., Rosenmai, A.K., Oskarsson, A., Bates, L., Figueiredo, R.S., Ibrahim, I., Wilson, C., Abdelkader, N.F., Jones, D.E., Blain, P.G., Wright, M.C., 2020a. The toxicity of the methylimidazolium ionic liquids, with a focus on M8OI and hepatic effects. *Food Chem. Toxicol.* 136, 111069.

Leitch, A.C., Abdelghany, T.M., Charlton, A., Grigalyte, J., Oakley, F., Borthwick, L.A., Reed, L., Knox, A., Reilly, W.J., Agius, L., Blain, P.G., Wright, M.C., 2020b. Renal injury and hepatic effects from the methylimidazolium ionic liquid M8OI in mouse. *Ecotoxicol. Environ. Saf.* 202, 110902.

Leitch, A.C., Ibrahim, I., Abdelghany, T.M., Charlton, A., Roper, C., Vidler, D., Palmer, J. M., Wilson, C., Jones, D.E., Blain, P.G., Wright, M.C., 2021. The methylimidazolium ionic liquid M8OI is detectable in human sera and is subject to biliary excretion in perfused human liver. *Toxicology* 459, 152854.

Leitch, A.C., Abdelghany, T.M., Charlton, A., Cooke, M., Wright, M.C., 2024. The Ionic Liquid 1-Octyl-3-Methylimidazolium (M8OI) Is Mono-Oxygenated by CYP3A4 and CYP3A5 in Adult Human Liver. Manuscript submitted.

Li, X., Ma, J., Wang, J., 2015. Cytotoxicity, oxidative stress, and apoptosis in HepG2 cells induced by ionic liquid 1-methyl-3-octylimidazolium bromide. *Ecotoxicol. Environ. Saf.* 120, 342–348.

Ma, J., Li, X., 2018. Insight into the negative impact of ionic liquid: a cytotoxicity mechanism of 1-methyl-3-octylimidazolium bromide. *Environ. Pollut.* 242, 1337–1345.

Markiewicz, M., Jungnickel, C., Cho, C.W., Stolte, S., 2015. Mobility and biodegradability of an imidazolium based ionic liquid in soil and soil amended with waste sewage sludge. *Environ. Sci. Process. Impacts* 17, 1462–1469.

Marroquin, L.D., Hynes, J., Dykens, J.A., Jamieson, J.D., Will, Y., 2007. Circumventing the Crabtree effect: replacing media glucose with galactose increases susceptibility of HepG2 cells to mitochondrial toxicants. *Toxicol. Sci.* 97, 539–547.

Orr, J.G., Leel, V., Cameron, G.A., Marek, C.J., Haughton, E.L., Elrick, L.J., Trim, J.E., Hawsworth, G.M., Halestrap, A.P., Wright, M.C., 2004. Mechanism of action of the antifibrogenic compound gliotoxin in rat liver cells. *Hepatology* 40, 232–242.

Poolakkalody, N.J., Thattantavide, A., Manisseri, C., 2022. Evaluating the biofuel potential of perennial grass, Pennisetum polystachion based on aqueous 1-ethyl, 3-methylimidazolium acetate ([EMIM][Ac]) pretreatment. *Biomass Conv. Bioref.* <https://doi.org/10.1007/s13399-021-02166-6>.

Probert, P.M., Chung, G.W., Cockell, S.J., Agius, L., Mosesso, P., White, S.A., Oakley, F., Brown, C.D., Wright, M.C., 2014. Utility of B-13 progenitor-derived hepatocytes in hepatotoxicity and genotoxicity studies. *Toxicol. Sci.* 137, 350–370.

Probert, P.M.E., Meyer, S.K., Alsaedi, F., Axon, A.A., Fairhall, E.A., Wallace, K., Charles, M., Oakley, F., Jowsey, P.A., Blain, P.G., Wright, M.C., 2015. An expandable donor-free supply of functional hepatocytes for toxicology. *Toxicology Research* 4, 203–222.

Probert, P.M., Leitch, A.C., Dunn, M.P., Meyer, S.K., Palmer, J.M., Abdelghany, T.M., Lakey, A.F., Cooke, M.P., Talbot, H., Wills, C., McFarlane, W., Blake, L.I., Rosenmai, A.K., Oskarsson, A., Figueiredo, R., Wilson, C., Kass, G.E., Jones, D.E., Blain, P.G., Wright, M.C., 2018. Identification of a xenobiotic as a potential environmental trigger in primary biliary cholangitis. *J. Hepatol.* 69, 1123–1135.

Prince, M.I., Chetwynd, A., Diggle, P., Jarner, M., Metcalf, J.V., James, O.F., 2001. The geographical distribution of primary biliary cirrhosis in a well-defined cohort. *Hepatology* 34, 1083–1088.

Stanley, L.A., Wolf, C.R., 2022. Through a glass, darkly? HepaRG and HepG2 cells as models of human phase I drug metabolism. *Drug Metab. Rev.* 54, 46–62.

Triger, D.R., 1980. Primary biliary cirrhosis: an epidemiological study. *Br. Med. J.* 281, 772–775.

Van de Loosdrecht, A.A., Beelen, R.H., Ossenkuppe, G.J., Broekhoven, M.G., Langenhuijsen, M.M., 1994. A tetrazolium-based colorimetric MTT assay to quantitate human monocyte mediated cytotoxicity against leukemic cells from cell lines and patients with acute myeloid leukemia. *J. Immunol. Methods* 174, 311–320.

Wallace, K., Marek, C.J., Hoppler, S., Wright, M.C., 2010a. Glucocorticoid-dependent transdifferentiation of pancreatic progenitor cells into hepatocytes is dependent on transient suppression of WNT signalling. *J. Cell Sci.* 123, 2103–2110.

Wallace, K., Flecknell, P.A., Burt, A.D., Wright, M.C., 2010b. Disrupted pancreatic exocrine differentiation and malabsorption in response to chronic elevated systemic glucocorticoid. *Am. J. Pathol.* 177, 1225–1232.

Wright, M.C., Issa, R., Smart, D.E., Trim, N., Murray, G.I., Primrose, J.N., Arthur, M.J., Iredale, J.P., Mann, D.A., 2001. Gliotoxin stimulates the apoptosis of human and rat hepatic stellate cells and enhances the resolution of liver fibrosis in rats. *Gastroenterology* 121, 685–698.